

DISTURBANCE OBSERVER-BASED ADAPTIVE NONSINGULAR TERMINAL SLIDING MODE CONTROL FOR FAULT-TOLERANT CONTROL OF QUAD-TILTROTOR EVTOL

Seonwoo Kim†, Taewon Yun , Donghoon Seo , Jinyoung Suk & Seungkeun Kim‡

Department of Aerospace Engineering, Chungnam National University, Daejeon, Republic of Korea

Abstract

As Urban Air Mobility (UAM) operates in complex and unpredictable environments, robust control strategies are crucial for handling model uncertainties, external disturbances such as urban wind gusts and potential actuator faults. To address these challenges, this paper proposes a Disturbance Observer-based Adaptive Nonsingular Terminal Sliding Mode Control (DOB-based ANTSMC). The proposed strategy utilizes a Disturbance Observer to effectively compensate for uncertainties and disturbances, while employing an adaptive law to mitigate chattering in the control input. Simulation results demonstrate that the proposed method achieves superior tracking performance and robustness compared to PID and Super-Twisting Algorithm (STA).

Keywords: Urban Air Mobility (UAM), Adaptive Control, Nonsingular Terminal SMC (NTSMC), Disturbance Observer (DOB), Fault Tolerance

1. Introduction

Recently, Urban Air Mobility (UAM) has emerged as a next-generation transportation system with the potential to overcome the limitations of conventional road transportation systems and significantly improve the efficiency of urban mobility. Notably, tiltrotor eVTOLs have emerged as a key UAM platform by combining VTOL capabilities with high-speed cruising efficiency [1]. However, their nonlinear aerodynamic coupling and limited control redundancy make them highly vulnerable to attitude degradation under actuator faults, especially compared to conventional UAVs [2].

Moreover, when operating in complex urban environments, they are exposed to unpredictable disturbances, such as sudden wind gusts between buildings, alongside unexpected actuator faults that can cause a severe loss of control. Therefore, designing robust and fault-tolerant control (FTC) strategies is essential [3, 2]. Sliding Mode Control (SMC) has been extensively studied in the aerospace field due to its strong robustness against model uncertainties and external disturbances [1, 4]. However, conventional SMC has two major limitations. First, the discontinuous nature of the control input induces high-frequency oscillations, known as chattering, which can cause actuator wear and degrade system stability. Second, it generally guarantees only asymptotic convergence, meaning the system state cannot reach the final equilibrium point in finite time [5].

Various approaches have been proposed to overcome these limitations. For instance, higher-order sliding mode control (HOSMC) mitigates chattering but often requires higher-order derivatives, thereby amplifying measurement noise and increasing tuning complexity [5, 6, 7]. Other chattering reduction techniques frequently result in a trade-off between robustness and tracking accuracy [5, 8]. Alternatively, Terminal Sliding Mode Control (TSMC) guarantees finite time convergence but is inherently limited by a singularity problem near the equilibrium point [9]. While Non-singular Terminal Sliding Mode Control (NTSMC) overcomes this limitation [10], suppressing large-amplitude disturbances with a single controller requires excessively high switching gains, leading to chattering [4].

Integrating a Disturbance Observer (DOB) mitigates this issue by actively estimating and compensating for lumped disturbances, allowing the switching gain to remain relatively low [11]. Nevertheless, the application of DOB-based adaptive NTSMC to tiltrotor eVTOLs under combined urban wind gusts, aerodynamic uncertainties, and actuator loss-of-effectiveness scenarios has underexplored.
This paper proposes a Disturbance Observer-based Adaptive Nonsingular Terminal Sliding Mode Control (DOB-based ANTSMC) strategy. The proposed control architecture integrates three key mechanisms: First, a nonsingular terminal sliding surface eliminates the singularity problem of conventional TSMC and ensures rapid finite time convergence. Second, an adaptive law adjusts the switching gain in real time based on the error state, maintaining robustness while minimizing chattering without prior knowledge of disturbance upper bounds [8]. Third, a DOB actively estimates and compensates for sudden environmental disturbances and actuator loss of effectiveness (LOE), significantly reducing the control effort required from the switching control term and enhancing overall robustness [11].
The main contributions of this paper are summarized as follows:

- A DOB-based ANTSMC framework is designed and applied to a quad-tiltrotor eVTOL operating in environments subject to urban wind gusts and aerodynamic uncertainties.
- Through the combination of the DOB and the adaptive law, finite time convergence is achieved while effectively suppressing chattering, even without prior knowledge of the disturbance upper bounds.
- The FTC performance under an actuator loss of effectiveness (LOE) scenario is verified via numerical simulations, and its mathematical stability is strictly proven based on Lyapunov theory.

2. Dynamics Modeling

2.1 Quad-tiltrotor eVTOL Flight Dynamics

Table 1 – Specification of Quad-Tiltrotor eVTOL

Specification	Mass	Wing Area	I_{xx}	I_{yy}	I_{zz}
Value	40 [kg]	1.885 [m^2]	8.2 [kg·m^2]	9.9 [kg·m^2]	19.724 [kg·m^2]

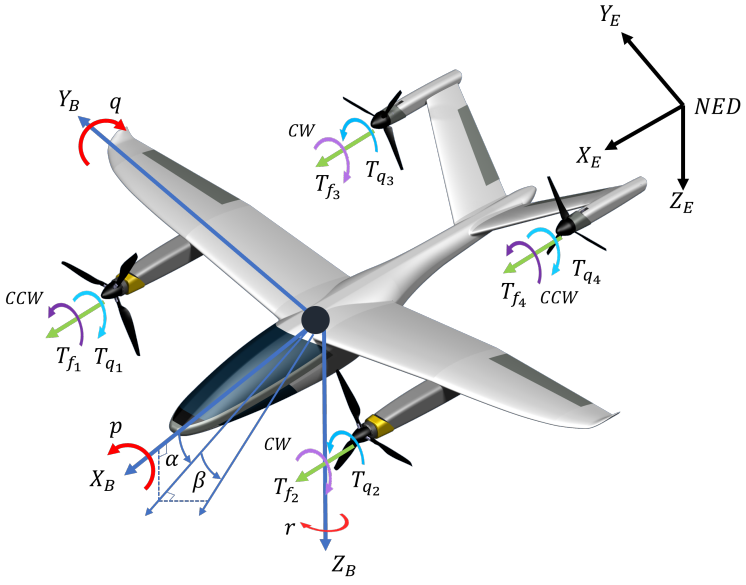


Figure 1 – Configuration of Quad-Tiltrotor eVTOL

The force and moment equations, incorporating aerodynamic effects and rotor thrusts, are defined as in Equations (1)-(6).

$$F_x = \frac{1}{2}\rho V^2 S C_X + (T_{f1} + T_{f2} + T_{f3} + T_{f4})\cos(\zeta) \tag{1}$$

$$F_y = \frac{1}{2}\rho V^2 S C_Y \tag{2}$$

$$F_z = \frac{1}{2}\rho V^2 S C_Z + (T_{f1} + T_{f2} + T_{f3} + T_{f4})\sin(\zeta) \tag{3}$$

$$M_x = \frac{1}{2}\rho V^2 S b C_l + (T_{f2} - T_{f1})\sin(\zeta)\delta_{y_{1,2}} + (T_{f4} - T_{f3})\sin(\zeta)\delta_{y_{3,4}} + (-T_{q1} + T_{q2} + T_{q3} - T_{q4})\cos(\zeta) \tag{4}$$

$$M_y = \frac{1}{2}\rho V^2 S C_m c + (T_{f1} + T_{f2})\sin(\zeta)\delta_{x_{1,3}} - (T_{f3} + T_{f4})\sin(\zeta)\delta_{x_{3,4}} \tag{5}$$

$$M_z = \frac{1}{2}\rho V^2 S b C_n + (T_{q1} - T_{q2} - T_{q3} + T_{q4})\sin(\zeta) \tag{6}$$

Here, ρ denotes the air density, V is the flight speed, S is the wing area, and ζ represents the rotor tilt angle. In addition, T_{fi} and T_{qi} denote the thrust and reaction torque of the i-th rotor, respectively. The nonlinear dynamic model of the quad-tiltrotor eVTOL is derived from its aerodynamic and dynamic parameters. Subject to external wind gusts, aerodynamic uncertainties, and actuator LOE faults, the system dynamics can be expressed in the following control-affine system:

$$\dot{x} = f(x) + g(x)u(t) + d(t) \tag{7}$$

where $f(x)$ represents the nominal nonlinear system dynamics, and $g(x)$ is the control effectiveness matrix. The term $d(t)$ denotes the lumped disturbance, accounting for aerodynamic uncertainties, urban wind gusts, and actuator LOE faults. State vector x and the control input vector u are defined as follows:

$$x = [u, v, w, p, q, r, \phi, \theta, \psi]^T \tag{8}$$

$$u = [\delta_{thr}, \delta_{ail}, \delta_{ele}, \delta_{rud}]^T \tag{9}$$

2.2 Actuator LOE Fault Model

Due to long-term operation or unexpected physical damage, a LOE fault may occur, where a specific rotor motor fails to generate the commanded thrust T_{ci}. The actual thrust T_{fi} generated by the rotor is modeled as follows:

$$T_{fi} = \eta_i T_{ci} \tag{10}$$

where η_i is the effectiveness factor of the rotor. $\eta_i = 1$ indicates a healthy, nominal state, while $0 < \eta_i < 1$ represents a partial loss of thrust fault. In this study, focusing on longitudinal control, we consider a scenario with simultaneous faults occurring in the forward rotors T_{f1} and T_{f2}. This condition results in an abrupt loss of the pitching moment M_y, inducing a severe nose-down instability. Consequently, this fault acts as a critical internal disturbance that significantly degrades overall control performance.

3. DOB-based ANTSMC Framework

This section proposes an integrated control framework to achieve robust longitudinal attitude control of the quad-tiltrotor, even in the presence of the lumped disturbances defined in Section 2. The proposed controller consists of two components: a linear DOB that estimates disturbances in real-time, and an Adaptive NTSMC designed to compensate for estimation errors and system nonlinearities.

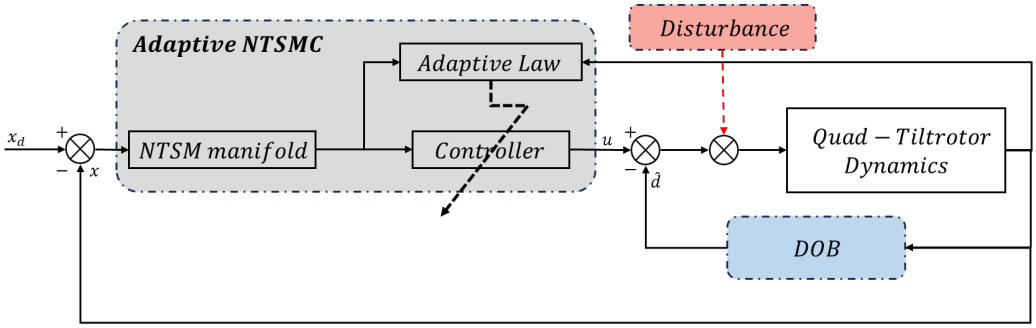


Figure 2 – Block diagram of the DOB-based ANTSMC

3.1 Disturbance Observer Design

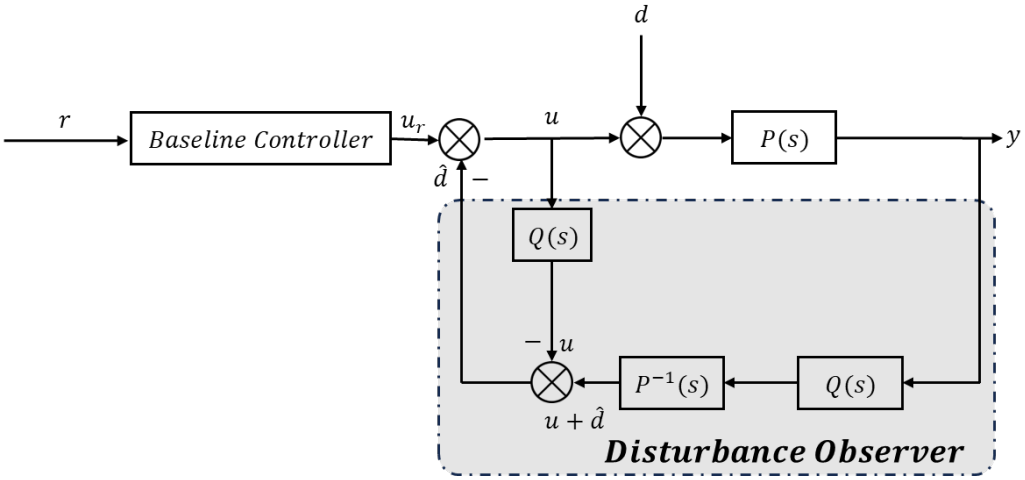


Figure 3 – Structure of the proposed DOB

Handling disturbances using an SMC alone requires excessively large switching gains, which inevitably induce severe chattering and impose physical strain on the rotor actuators. To prevent this and maximize control robustness, this study integrates a DOB within the control loop to estimate and actively compensate for disturbances in real time. Crucially, DOB offers the significant advantage of effectively suppressing time-varying disturbances while maintaining the normal performance of the baseline control system in the absence of disturbances.

The nominal linear model of the longitudinal pitch dynamics, denoted as $P_n(s)$, and the Q-filter $Q(s)$, which is designed for sensor noise filtering and the practical implementation of the nominal model's inverse $P_n^{-1}(s)$, are defined as follows, respectively:

$$P_n(s) = \frac{\theta}{\delta_{ele}} = \frac{C_{M_{\delta E}}}{I_{yy}s^2} \tag{11}$$

$$Q(s) = \frac{\omega_n^2}{s^2 + 2\zeta\omega_n s + \omega_n^2} \tag{12}$$

Based on the structure shown in Fig. 3, the DOB actively estimates the disturbance using $P_n^{-1}(s)$ and $Q(s)$ to generate a direct compensation input for the system. Accordingly, the disturbance estimate $\hat{d}$ and the required control input u_{DOB} to reject this disturbance are formulated as follows:

$$\hat{d} = Q(s)(P_n^{-1}(s)\theta(s) - u_c(s)), \quad u_{DOB} = -\hat{d} \tag{13}$$

Through this compensation mechanism, the DOB actively rejects the majority of the lumped disturbances. Consequently, the baseline controller only needs to handle the estimation error $\tilde{d} = d - \hat{d}$ and any residual uncertainties. This significantly reduces the required switching gain, thereby alleviating chattering while preserving robustness.

3.2 Adaptive NTSMC Design

To overcome the singularity problem inherent in conventional TSMC and ensure finite time convergence, the sliding surface of the proposed SMC is designed as follows, defining the tracking error as $e = \theta - \theta_{cmd}$ [10].

$$s = e + \frac{1}{\beta}|\dot{e}|^{p/q}\,\mathrm{sign}(\dot{e}) + \int \lambda e dt \tag{14}$$

Here, $\beta > 0$ and $\lambda > 0$, and p and q are positive odd integers satisfying $1 < p/q < 2$. Taking the time derivative of the sliding surface and defining the nonlinear term as $\Gamma = \frac{1}{\beta}\frac{p}{q}|\dot{e}|^{(p/q)-1}$, the system dynamics are expanded as follows.

$$\dot{s} = \dot{e} + \Gamma\ddot{e} + \lambda e = \dot{e} + \Gamma(F(x) + G_1(x)u - \ddot{r} + d(t)) + \lambda e \tag{15}$$

The total control input required to force the system states onto the sliding surface $s = 0$ consists of the sum of the equivalent and adaptive control input.

$$u = u_{eq} + u_{adaptive} \tag{16}$$

Here, the equivalent control input is designed to guarantee system stability using the nonlinear system matrices derived from the model. The adaptive control input is designed to compensate for model uncertainties and disturbances, incorporating adaptive gains $\hat{h}_i$ based on the state variables as follows:

$$u_{eq} = G_1(x)^{-1}(\ddot{r} - F(x) - \Gamma^{-1}\dot{e} - \Gamma^{-1}\lambda e - \Gamma^{-1}K\,\mathrm{sign}(s)) \tag{17}$$

$$u_{adaptive} = -G_1(x)^{-1}\left(\hat{h}_0 + \hat{h}_1|x| + \hat{h}_2|\dot{x}|^2\right)\mathrm{sign}(s) \tag{18}$$

To prove the stability of the proposed controller, the following Lyapunov candidate function V is defined [8].

$$V = \frac{1}{2}s^2 + \frac{1}{2}\sum_{i=0}^{2}\frac{1}{\gamma_i}\tilde{h}_i^2 \tag{19}$$

where $\tilde{h}_i = h_i - \hat{h}_i$ represents the estimation error of the adaptive gains, and γ_i is a positive adaptive gain constant. Differentiating V with respect to time and substituting the previously designed control input u results in the following:

$$\dot{V} = -K|s| + \Gamma d(t)s - \Gamma\left(\hat{h}_0 + \hat{h}_1|x| + \hat{h}_2|\dot{x}|^2\right)|s| - \sum_{i=0}^{2}\frac{1}{\gamma_i}\tilde{h}_i\dot{\hat{h}}_i \tag{20}$$

Using the assumed upper bound of the disturbance $|d(t)| \le h_0 + h_1|x| + h_2|\dot{x}|^2$, the inequality can be rewritten as

$$\begin{aligned}\dot{V} &\le -K|s| + \Gamma(h_0 + h_1|x| + h_2|\dot{x}|^2)|s| - \Gamma(\hat{h}_0 + \hat{h}_1|x| + \hat{h}_2|\dot{x}|^2)|s| - \sum_{i=0}^{2}\frac{1}{\gamma_i}\tilde{h}_i\dot{\hat{h}}_i \\ &= -K|s| + \tilde{h}_0\left(\Gamma|s| - \frac{1}{\gamma_0}\dot{\hat{h}}_0\right) + \tilde{h}_1\left(\Gamma|x||s| - \frac{1}{\gamma_1}\dot{\hat{h}}_1\right) + \tilde{h}_2\left(\Gamma|\dot{x}|^2|s| - \frac{1}{\gamma_2}\dot{\hat{h}}_2\right)\end{aligned} \tag{21}$$

To guarantee negative definiteness while preventing parameter drift near the sliding surface, the adaptive laws are defined as follows:

$$\dot{\hat{h}}_0 = \begin{cases}\gamma_0\Gamma|s| & \text{if } |s| \ge \varepsilon \\ 0 & \text{if } |s| < \varepsilon\end{cases} \tag{22}$$

$$\dot{\hat{h}}_1 = \begin{cases}\gamma_1\Gamma|x||s| & \text{if } |s| \ge \varepsilon \\ 0 & \text{if } |s| < \varepsilon\end{cases} \tag{23}$$

$$\dot{\hat{h}}_2 = \begin{cases}\gamma_2\Gamma|\dot{x}|^2|s| & \text{if } |s| \ge \varepsilon \\ 0 & \text{if } |s| < \varepsilon\end{cases} \tag{24}$$

Where $\varepsilon > 0$ represents the boundary layer width. Substituting these adaptive laws into the Lyapunov derivative, the complete cancellation of the estimation error terms occurs for $|s| \geq \varepsilon$.

$$\dot{V} \leq -K|s| \leq 0 \tag{25}$$

Consequently, since $\dot{V} \leq 0$ is guaranteed outside the deadzone ($|s| \geq \varepsilon$), it is mathematically proven that the proposed controller ensures robust stability, driving the state variables to the boundary layer of the sliding surface within a finite time.

4. Simulation

4.1 Simulation Setup and Scenarios

To validate the performance of the proposed DOB-based ANTSMC framework, flight simulations were performed using a 6-degree-of-freedom (6-DOF) quad-tiltrotor dynamic model in the MATLAB/Simulink environment. The physical parameters of the aircraft used in the simulation correspond to the specifications detailed in Table 1. To objectively evaluate the performance of the proposed method, a conventional PID controller and a Super-Twisting Algorithm (STA)-based SMC were selected as comparative baselines [12, 13].

To replicate the uncertainties likely to be encountered in actual urban flight environments, aerodynamic parameter uncertainties and an urban wind gust model were introduced as baseline disturbances across all simulations. Additionally, to verify the FTC capabilities of the proposed controller, the following two simulation scenarios were established:

- **Scenario 1:** Evaluates the nominal tracking performance in the presence of time-varying disturbances and model uncertainties throughout the entire flight.
- **Scenario 2:** Under the same disturbance conditions as Scenario 1, this scenario assumes a simultaneous 30% loss of effectiveness in the two forward rotors at $t = 30$ s, which directly impacts the longitudinal control.

4.2 Results and Discussion

The simulation results under complex disturbances and actuator fault conditions are presented in Figs. 4–6 and Tables 2–3.

Fig. 4 illustrates the simulation results for Scenario 1, which involves urban wind gusts and model uncertainties. Regarding pitch angle tracking, all three controllers successfully follow the reference trajectory. Notably, the proposed ANTSMC exhibits the most stable response and the lowest error amplitude. Furthermore, the comparison of the ruddervator control inputs demonstrates that the STA exhibits severe high-frequency chattering, whereas the ANTSMC generates a smooth control action while maintaining strong robustness. In the sliding surface plot, the ANTSMC rapidly converges to the sliding manifold and remains stable, whereas the STA exhibits a slower convergence rate with minor chattering.

Regarding the disturbance estimation performance of the DOB, a comparison between the actual disturbance d and the estimated disturbance $\hat{d}$ shows an estimation error during the initial transient response period ($t \approx 0 \sim 15$ s). This error is attributed to the temporary discrepancy between the nominal model and the actual plant dynamics during reference maneuvering. However, after $t \approx 20$ s, the DOB accurately tracks the wind gust profile. This active compensation provides the basis for maintaining the switching gain of the ANTSMC at a low level.

Fig. 5 presents the simulation results for Scenario 2, where an actuator fault is introduced at $t = 30$ s, in addition to the disturbance conditions of Scenario 1. Even at the exact moment of fault occurrence, the ANTSMC minimizes error fluctuations and rapidly recovers to the reference trajectory within a finite time. This rapid recovery is achieved by immediately compensating for the loss of pitching moment induced by the fault, which is facilitated by combining the active disturbance compensation of the DOB with the adaptive law.

Fig. 6 compares the phase portraits of the STA and the proposed ANTSMC. While the trajectory of the STA exhibits a broader path during its convergence to the origin ($e = 0, \dot{e} = 0$), the ANTSMC

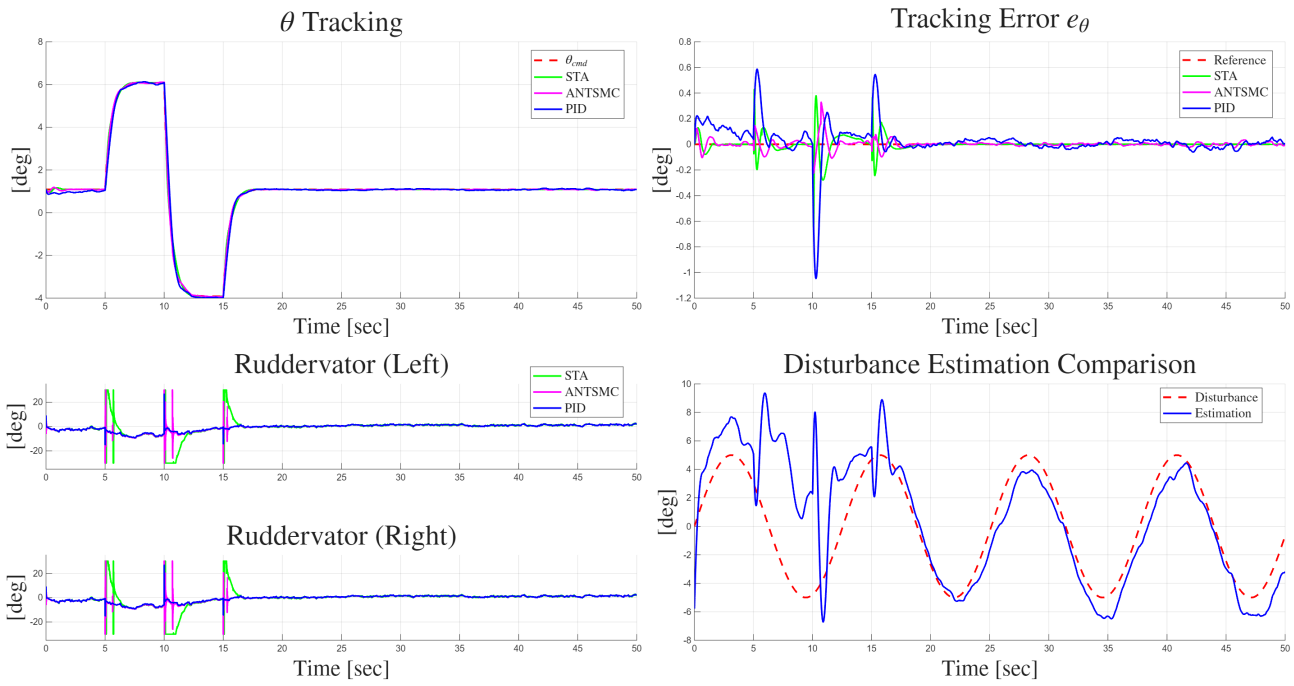


Figure 4 – Simulation results of PID, STA and ANTSMC (Scenario 1)

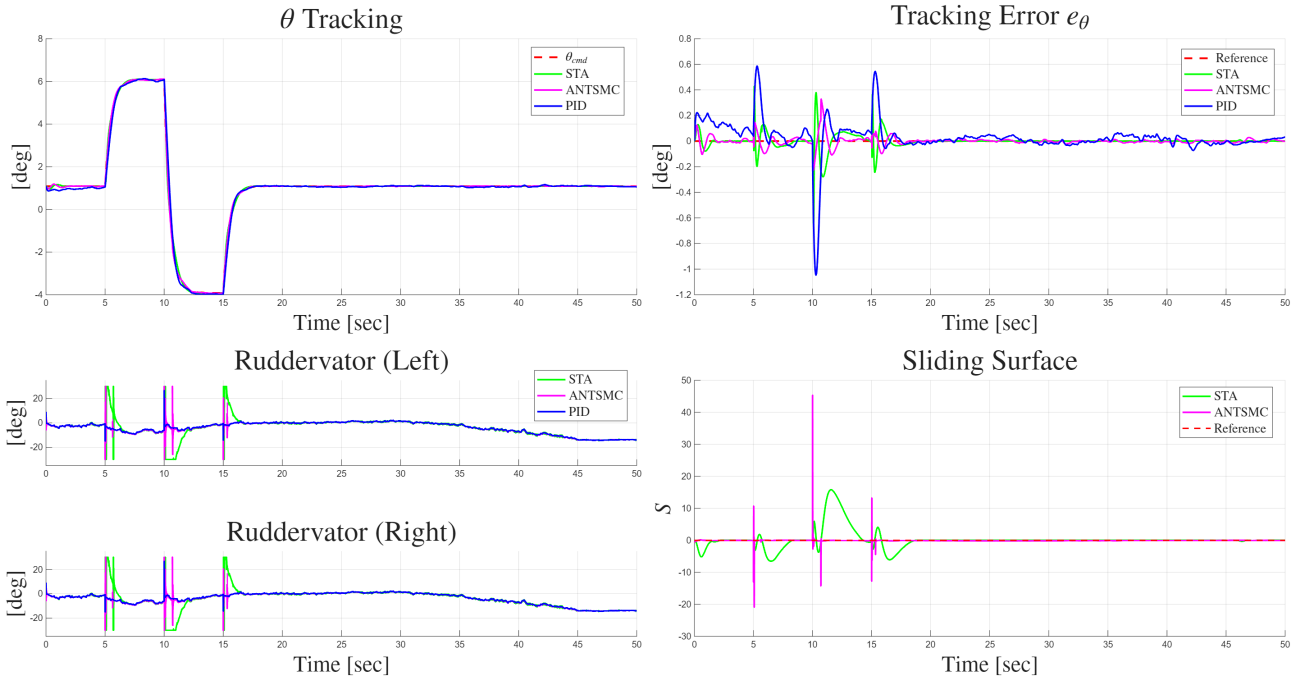
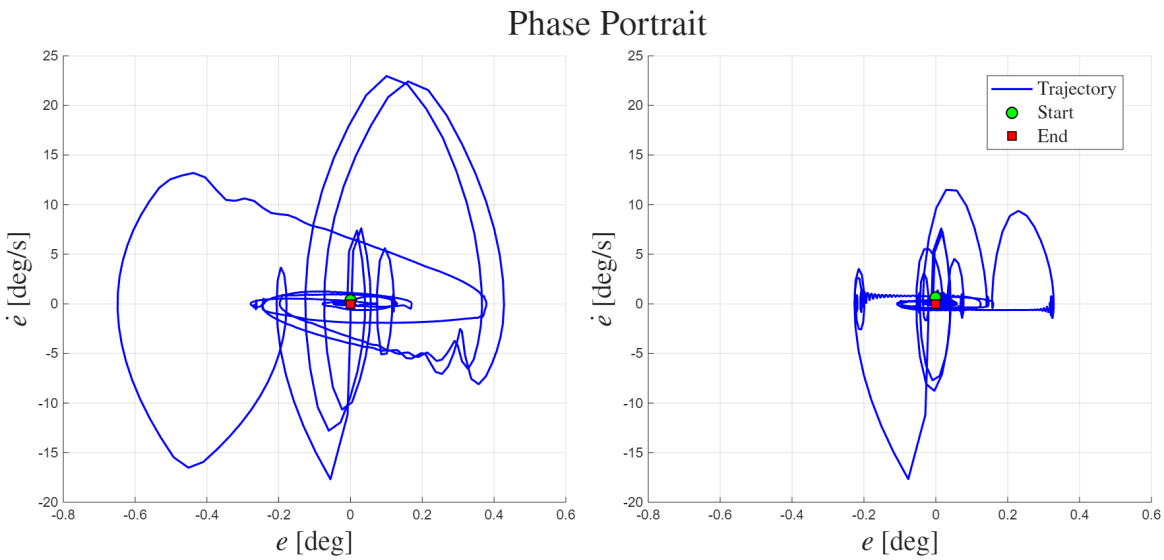


Figure 5 – Simulation results of PID, STA and ANTSMC (Scenario 2)



(a) STA Phase Portrait (b) ANTSMC Phase Portrait

Figure 6 – Phase Portraits of the Tracking Error

converges to the origin rapidly and stably. This substantiates that the Lyapunov stability theory proven in Section 3 is mathematically valid in the numerical simulations as well.

To quantitatively compare the tracking precision and control efficiency of each controller, the Root Mean Square Error (RMSE), Mean Absolute Error (MAE), and Total Variation (TV) were computed. The corresponding performance metrics are defined as follows:

$$\text{MAE} = \frac{1}{N}\sum_{i=1}^{N}|e_i|, \quad \text{TV} = \sum_{i=1}^{N-1}|u_{i+1}-u_i| \tag{26}$$

Table 2 – Quantitative Performance Comparison (Scenario 1)

Performance / Controller	RMSE [deg]		MAE [deg]		TV [deg]	
	w/o DOB	w/ DOB	w/o DOB	w/ DOB	w/o DOB	w/ DOB
ANTSMC	0.0468	0.0368	0.0343	0.0183	1304.65	1606.10
STA	0.1258	0.0556	0.0420	0.0199	2986.28	3844.32
PID	0.2234	0.1332	0.1817	0.0621	324.09	334.20

Table 3 – Quantitative Performance Comparison (Scenario 2)

Performance / Controller	RMSE [deg]		MAE [deg]		TV [deg]	
	w/o DOB	w/ DOB	w/o DOB	w/ DOB	w/o DOB	w/ DOB
ANTSMC	0.0447	0.0366	0.0308	0.0179	1330.71	1628.17
STA	0.1258	0.0556	0.0422	0.0201	3884.20	4495.28
PID	0.2487	0.1333	0.2040	0.0620	320.06	329.09

Tables 2 3, and Fig. 7 present the overall quantitative comparison results, with Fig. 7 visually highlighting the significant RMSE reduction achieved by applying the DOB. The analysis indicates that the proposed ANTSMC achieved the highest tracking precision in both scenarios. In Scenario 1, the ANTSMC reduced the RMSE by approximately 72.4% compared to the PID controller and by 33.8%

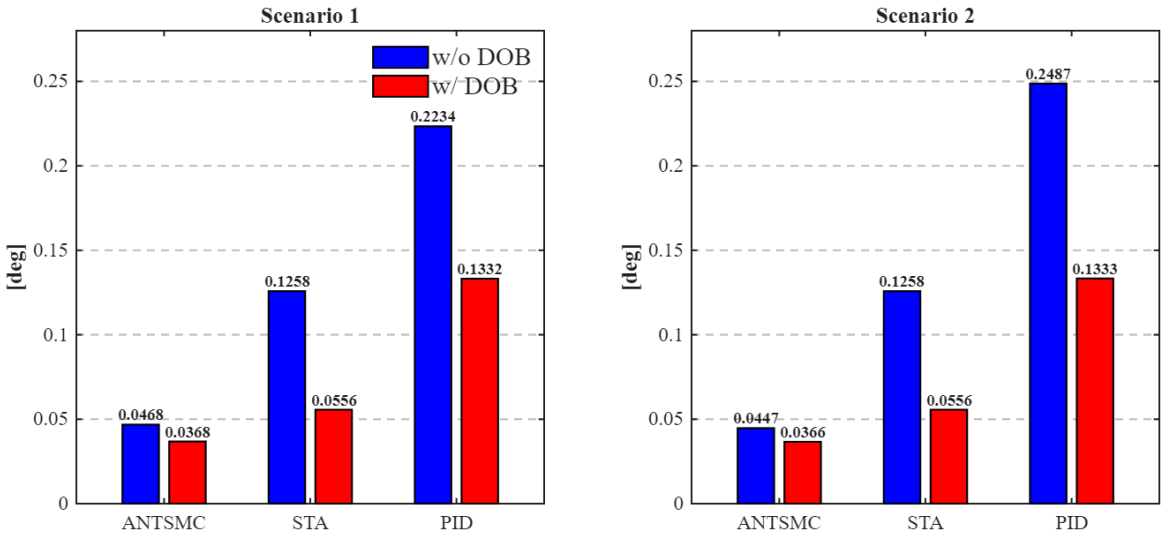


Figure 7 – RMSE Comparison of Controllers (Scenario 1 & 2)

compared to the STA. In Scenario 2, it reduced the RMSE by approximately 72.5% compared to the PID, demonstrating exceptional FTC performance.

Notably, the RMSE and MAE of the ANTSMC were nearly identical between Scenario 1 and Scenario 2. This is interpreted as the complementary action of the proactive disturbance compensation by the DOB and the compensation of residual uncertainties by the adaptive law, which effectively suppresses any degradation in control performance despite the fault occurrence.

Regarding control efficiency (TV), although the PID controller recorded the lowest TV among the three controllers, its significantly higher RMSE and MAE illustrate a clear trade-off between tracking precision and control effort. In contrast, the ANTSMC reduced the TV by approximately 63.8% compared to the STA in Scenario 2 while simultaneously achieving the highest tracking precision. This confirms its ability to maximize tracking performance while minimizing the actuation effort exerted on the rotor actuators.

5. Conclusion

This paper proposed a DOB-based ANTSMC framework to ensure the flight safety and reliability of quad-tiltrotor eVTOL aircraft operating in urban environments. The proposed control architecture overcomes the limitations of conventional methods by integrating three core mechanisms. First, by designing a nonsingular terminal sliding surface, the singularity problem inherent in traditional TSMC was eliminated, and finite time error convergence was guaranteed. Second, a DOB integrated into the control loop estimated and actively compensated for lumped disturbances—such as aerodynamic uncertainties, urban wind gusts, and actuator LOE faults—in real time. Third, by introducing an adaptive law that adjusts in real time according to the tracking error, chattering was effectively mitigated while maintaining robustness, even without prior knowledge of the disturbance upper bounds.

The effectiveness of the proposed method was verified through MATLAB/Simulink-based longitudinal flight simulations. Under a complex scenario involving urban wind gusts and a 30% loss of effectiveness in the forward rotors, the proposed DOB-based ANTSMC demonstrated exceptional tracking precision and FTC performance, reducing the RMSE by approximately 72.5% compared to the PID controller under the same DOB conditions. Furthermore, when compared to the STA, the proposed method reduced the TV of the control input by approximately 63.8%. This confirmed that the proposed framework can effectively maintain tracking performance while minimizing the actuation effort required by exertion on the actual rotor actuators.

The results of this study can be utilized as a core control technology to realize the safe urban flight of UAM vehicles, even under complex weather conditions and unexpected system faults. In future work, we plan to extend the proposed longitudinal control framework to lateral and directional (Lateral/Directional) dynamics and apply it to a full 6-DOF flight model to verify its fault-tolerant performance during 3D complex maneuvers and transition flight phases. Additionally, subsequent research

will involve Processor-in-the-Loop (PIL) simulations and actual flight tests to validate the computational efficiency and real-world applicability of the proposed control strategy on an embedded flight controller.

6. Contact Author Email Address

‡ skim78@cnu.ac.kr (corresponding author)
† jerkim@o.cnu.ac.kr

7. Copyright Statement

The authors confirm that they, and/or their company or organization, hold copyright on all of the original material included in this paper. The authors also confirm that they have obtained permission, from the copyright holder of any third party material included in this paper, to publish it as part of their paper. The authors confirm that they give permission, or have obtained permission from the copyright holder of this paper, for the publication and distribution of this paper as part of the ICAS proceedings or as individual off-prints from the proceedings.

Acknowledgement

This work was supported by the National Research Foundation of Korea (NRF) grant funded by the Korea government(MSIT)(No. 2021R1A5A1031868).

References

[1] Shen S, Xu J, Luo M and Zhou G. Adaptive neural network extended state observer-based finite time convergent sliding mode control for a quad tiltrotor UAV. *IEEE Transactions on Aerospace and Electronic Systems*, Vol. 59, No. 5, pp 6360-6373, 2023.

[2] Mousaei M, Geng J, Keipour A, Bai D and Scherer S. Design, modeling and control for a tilt-rotor VTOL UAV in the presence of actuator failure. *Proc IEEE/RSJ International Conference on Intelligent Robots and Systems (IROS)*, pp 4310-4317, 2022.

[3] Ahn CI, Kim Y and Kim H. Adaptive sliding mode controller design for fault tolerant flight control system. *Proc AIAA Guidance, Navigation, and Control Conference and Exhibit*, Keystone, Colorado, AIAA 2006-6089, 2006.

[4] Hou Z, Lu P and Tu Z. Nonsingular terminal sliding mode control for a quadrotor UAV with a total rotor failure. *Aerospace Science and Technology*, Vol. 98, Art. no. 105716, 2020.

[5] Lee H and Utkin VI. Chattering suppression methods in sliding mode control systems. *Annual Reviews in Control*, Vol. 31, No. 2, pp 179-188, 2007.

[6] Levant A. Sliding order and sliding accuracy in sliding mode control. *International Journal of Control*, Vol. 58, No. 6, pp 1247-1263, 1993.

[7] Levant A. Higher-order sliding modes, differentiation and output-feedback control. *International Journal of Control*, Vol. 76, No. 9-10, pp 924-941, 2003.

[8] Wan L, Chen G, Sheng M, Zhang Y and Zhang Z. Adaptive chattering-free terminal sliding-mode control for full-order nonlinear system with unknown disturbances and model uncertainties. *International Journal of Advanced Robotic Systems*, Vol. 17, No. 3, Art. no. 1729881420925295, 2020.

[9] Tang P, Zhang F, Ye J and Lin D. An integral TSMC-based adaptive fault-tolerant control for quadrotor with external disturbances and parametric uncertainties. *Aerospace Science and Technology*, Vol. 109, Art. no. 106415, 2021.

[10] Feng Y, Yu X and Man Z. Non-singular terminal sliding mode control of rigid manipulators. *Automatica*, Vol. 38, No. 12, pp 2159-2167, 2002.

[11] Wang B, Yu X, Mu L and Zhang Y. Disturbance observer-based adaptive fault-tolerant control for a quadrotor helicopter subject to parametric uncertainties and external disturbances. *Mechanical Systems and Signal Processing*, Vol. 120, pp 727-743, 2019.

[12] Moreno JA and Osorio M. Strict Lyapunov functions for the super-twisting algorithm. *IEEE Transactions on Automatic Control*, Vol. 57, No. 4, pp 1035-1040, 2012.

[13] Munoz F, Gonzalez-Hernandez I, Salazar S, Espinoza ES and Lozano R. Second order sliding mode controllers for altitude control of a quadrotor UAS: Real-time implementation in outdoor environments. *Neurocomputing*, Vol. 233, pp 61-71, 2017.